



Original Article

Integrative analysis of metabolome and transcriptome provides new insights into functional components of *Lilii Bulbus*Wenjun Wei^{a,b}, Tao Guo^{a,b,*}, Wenguang Fan^c, Mengshan Ji^{a,b}, Yu Fu^{a,b}, Conglong Lian^{a,b}, Suiqing Chen^{a,b}, Wenjing Ma^c, Wenfang Ma^d, Shuying Feng^{e,*}^a School of Pharmacy, Henan University of Chinese Medicine, Zhengzhou 450046, China^b Henan Engineering Research Center of Medicinal and Edible Chinese Medicine Technology, Zhengzhou 450046, China^c School of Life Science and Engineering, Lanzhou University of Technology, Lanzhou 730050, China^d Lanzhou Shibai Agricultural Biotechnology Co., Ltd., Lanzhou 730050, China^e Medical College, Henan University of Chinese Medicine, Zhengzhou 450046, China

ARTICLE INFO

Article history:

Received 3 July 2023

Revised 1 September 2023

Accepted 9 October 2023

Available online 29 January 2024

Keywords:

Lilium brownii F. E. Brown var. *viridulum*

Baker

Lilium davidii var. *willmottiae* (E. H. Wilson)

Raffill

Lilium lancifolium Thunb.

metabolome

transcriptome

ABSTRACT

Objective: *Lilium brownii* var. *viridulum* (LB) and *L. lancifolium* (LL) are the main sources of medicinal lily (*Lilii Bulbus*, Baihe in Chinese) in China. However, the functional components of these two species responsible for the treatment efficacy are yet not clear. In order to explore the therapeutic material basis of *Lilii Bulbus*, we selected *L. davidii* var. *willmottiae* (LD) only used for food as the control group to analyze the differences between LD and the other two (LB and LL).

Methods: Metabolome and transcriptome were carried out to investigate the differences of active components in LD vs LB and LD vs LL. Data of metabolome and transcriptome was analysed using various analysis methods, such as principal component analysis (PCA), hierarchical cluster analysis (HCA), and so on. Differentially expressed genes (DEGs) were enriched through KEGG and GO enrichment analysis. **Results:** The PCA and HCA of the metabolome indicated the metabolites were clearly separated and varied greatly in LL and LB contrasted with LD. There were 318 significantly differential metabolites (SDMs) in LD vs LB group and 298 SDMs in LD vs LL group. Compared with LD group, the significant up-regulation of steroidal saponins and steroidal alkaloids were detected both in LB and LL groups, especially in LB group. The HCA of transcriptome indicated that there was significant difference in LB vs LD group, while the difference between LL and LD varied slightly. Additionally, 47 540 DEGs in LD vs LB group and 18 958 DEGs in LD vs LL group were identified. Notably, CYP450s involving in the biosynthesis of steroidal saponins and steroidal alkaloids were detected, and comparing with LD, CYP724, CYP710A, and CYP734A1 in LB and CYP90B in LL were all up-regulated.

Conclusion: This study suggested that steroidal saponins and steroidal alkaloids maybe the representative functional components of *Lilii Bulbus*, which can provide new insights for *Lilii Bulbus* used in the research and development of classic famous formula.

© 2024 Tianjin Press of Chinese Herbal Medicines. Published by ELSEVIER B.V. This is an open access article under the CC BY-NC-ND license (<http://creativecommons.org/licenses/by-nc-nd/4.0/>).

1. Introduction

Lilium genus of Liliaceae family consists 110 species, mainly distributed in temperate regions of the northern hemisphere, such as Eastern Asia, Europe, and North America (Zhou, An, & Huang, 2021; Wu et al., 2022; Yang et al., 2023). China is considered to be the global diversity center of *Lilium* with 55 species and 32 varieties (Zhou, An, & Huang, 2021; Liang et al., 2022). Jiangsu Yixing, Hunan Shaoyang, Gansu Lanzhou and Zhejiang Huzhou have a long history of lily (*Lilii Bulbus*, Baihe in Chinese) cultivation and they also

become the “four major lily producing areas” in China. The bulbs of lily have been regularly consumed as both food and medicine (Munafò & Gianfagna, 2015). *Chinese Pharmacopoeia* stipulates that *Lilium lancifolium* Thunb. (LL), *L. brownii* F. E. Brown var. *viridulum* Baker (LB) and *L. pumilum* DC. (LP) are sources of medicinal *Lilii Bulbus* in traditional Chinese medicine to treat palpitations, insomnia and hemoptysis (Chinese Pharmacopoeia Commission, 2020). Why does *Chinese Pharmacopoeia* stipulate these three kinds of *Lilii Bulbus* and which ingredients play a major role in drug efficacy in these plants? Previously phytochemical studies showed that *Lilii Bulbus* mainly contained steroidal saponins, alkaloids, phenolic glycerides, polysaccharides and so on. (Mimaki & Sashida, 1990; Zhou et al., 2012; Esposito et al., 2013; Matsuo, Takaku, &

* Corresponding authors.

E-mail addresses: gt010010@163.com (T. Guo), fsy@hactcm.edu.cn (S. Feng).

Mimaki, 2015; Munafo & Gianfagna, 2015; Zhou, An, & Huang, 2021). Pharmacological investigations indicated that *Lilii Bulbus* had good effects in anti-fatigue, anti-depression, anti-tumor, hypoglycemic, anti-oxidation, immune regulation, insomnia and so on (Munafo & Gianfagna, 2015; Di et al., 2020; Sim et al., 2020; Tang et al., 2021; Zhou, An, & Huang, 2021; Si et al., 2022a; Si et al., 2022b). However, the chemical compositions of *Lilii Bulbus* responsible for the reported biological activity have not been identified.

In order to further explore the bioactive components of *Lilii Bulbus*, the fresh bulbs of *L. davidii* var. *willmottiae* (E. H. Wilson) Raffill (LD) used only for food and medicinal lily (LL and LB) are used as experimental materials (Fig. 1). Among the three kinds of *Lilii Bulbus* prescribed in *Chinese Pharmacopoeia*, LL and LB account for 98% in the market circulation and become the main sources of *Lilii Bulbus* (Qin et al., 2022). The bulbs of LD are an extremely sweet vegetable without any bitter taste, which is also the only edible sweet lily (Wang, Wang, Niu, Huang, & Zhang, 2018). We have used a system biology approach based on the differential metabolomics and transcriptomics between medicinal (LB, LL) and edible (LD) lilies to clarify the functional components of *Lilii Bulbus*.

2. Materials and methods

2.1. Plant materials

Fresh bulbs of *L. davidii* var. *willmottiae* (LD), *L. lancifolium* (LL), and *L. brownii* var. *viridulum* (LB) were successively collected from Gansu Lanzhou (36°03' N, 103°40' E), Jiangsu Yixing (31°35' N, 119°82' E), and Hunan Shaoyang (27°14' N, 111°28' E) in September 2019, which were identified by Professor Tao Guo of Henan University of Chinese Medicine. These three lilies collected from different planting areas are all two-year old. All fresh bulbs were frozen in liquid nitrogen and stored at -80°C for RNA and metabolite extraction. In this study, three biological replicates were used in the experiments.

2.2. Sample extraction

All fresh bulbs were freeze-dried in vacuum placed in a freeze-drying machine (Scientz-100F, Ningbo Scientz Biotechnology Co., Ltd., Ningbo, China) and grinded for 1.5 min with grinding instrument (MM 400, Retsch, Dusseldorf, North Rhine Westphalia, Germany) to powder state. A total of 100 mg of powder was weighed and dissolved in 1.2 mL of 70% methanol, the solution was vortexed every 30 min for a total of six times, and then placed the samples in a 4°C refrigerator overnight. After centrifugation

(12 000 r/min, 10 min) with refrigerated centrifuge (5430R, Eppendorf, Hamburg, Germany), the supernatant was filtered using an microporous membrane ($0.22\ \mu\text{m}$) and stored in the injection bottle for UPLC-MS/MS analysis.

2.3. Analysis conditions of chromatography-mass spectrometry

A UPLC-MS/MS system (UPLC, SHIMADZU Nexera X2; MS/MS, Applied Biosystems 4500 QTRAP) was employed to analyze the sample. UPLC conditions: chromatographic column, Agilent SB-C₁₈ (100 mm × 2.1 mm, 1.8 μm , AB SCIEX, Foster City, CA, USA); mobile phase, A: water (0.1% formic acid), B: acetonitrile (0.1% formic acid); gradient program, 0–9 min, 95:5 to 5:95, volume ratio of A and B; 9–10 min, 5:95, volume ratio of A and B; 10–11 min, 5:95 to 95:5, volume ratio of A and B; 11–14 min, 95:5, volume ratio of A and B; flow rate: 0.35 mL/min; column temperature: 40°C ; injection volume: 4 μL . Linear ion hydrazine-flight time (LIT) and triple quadrupole (QQQ) scanning were obtained on triple quadrupole linear ion trap mass spectrometer (QTRAP), AB4500 QTRAP UPLC/MS/MS system, with positive ion and negative ion modes, which was equipped with ESI Turbo ion spray interface. The operation parameters of ESI source were set as follows: ion source, turbine spray; source temperature 550°C ; ion spray voltage (IS) 5 500 V (positive ion mode)/ $-4\ 500\ \text{V}$ (negative ion mode). The ion source gas I (GSI), gas II (GSII) and curtain gas (CUR) were set to 345, 414 and 172 kPa, respectively, and the collision induced ionization parameter was adjusted to high. The instrument tuning and mass calibration were applied in QQQ and LIT modes by using 10 and 100 $\mu\text{mol/L}$ polypropylene glycol solution, respectively. The QQQ scan used multiple reaction monitoring (MRM) mode with the collision gas (nitrogen) being medium. Declustering potential (DP) and collision energy (CE) of each MRM ion pair were completed after further optimization of DP and CE. A specific set of MRM ion pairs was monitored at each period based on the metabolites eluted.

2.4. Qualitative and quantitative principles of metabolites

The qualitative analysis of the metabolite data was carried out according to the secondary mass spectrum information based on the MWDB database (Metware Biotechnology Co., Ltd., Wuhan, China) (Wei et al., 2013; Thévenot, Roux, Xu, Ezan, & Junot, 2015). The metabolite quantification was completed by using the MRM mode of triple quadrupole mass spectrometry. After obtaining the mass spectrum analysis data of metabolites, the peak areas of all mass spectrum peaks were integrated. Then, the mass spectrum peaks of the same metabolite in different samples were inte-



Fig. 1. Morphology of three species of *Lilium* (A: *L. davidii* var. *willmottiae*; B: *L. brownii* var. *viridulum*; C: *L. lancifolium*).

grated and corrected. The quality control (QC) sample was prepared by mixing the sample extracts to analyze the repeatability of the samples under the same processing method. The high stability of the instrument provided an important guarantee for the repeatability and reliability of data. Principal component analysis (PCA) was an unsupervised pattern recognition method for multi-dimensional data statistical analysis, which can reveal the internal structure of multiple variables through a few principal components. The metabolite content data was normalized by unit variance scaling (UV). The hierarchical cluster analysis (HCA) of the metabolite accumulation patterns among different samples was performed by the R software pheatmap package to draw a heat map. Significantly different metabolites between different groups were determined based on $VIP \geq 1$ and $|\log_2 FC| \geq 1$. Volcano plot was used to quickly view the difference in the accumulated level of metabolites in different samples and the statistical significance of the difference.

2.5. RNA isolation and transcriptome sequencing

Total RNA was extracted using the RNeasy Pure Plant Kit (Tiangen, China) according to the manufacturer's instructions. RNA purity and integrity were assessed using the NanoPhotometer® spectrophotometer (IMPLEN, CA, USA) and the RNA Nano 6000 Assay Kit of the Bioanalyzer 2100 system (Agilent Technologies, CA, USA), respectively. RNA samples that met the quality requirements were used to construct a sequencing library and then sequenced on the Illumina novaseq 6000 platform. The clustering of the index-coded samples was performed on a cBot Cluster Generation System using TruSeq PE Cluster Kit v3-cBot-HS (NovaSeq 6000 System, Illumina, California, USA) according to the manufacturer's instructions. The original data was filtered to remove low-quality reads with adapters using fastp v0.19.3. All subsequent analyses were based on clean reads. The clean reads were *de novo* assembled using StringTie v1.3.4d to obtain high-quality transcript sequences. Fragments per kilobase of exon per million fragments mapped (FPKM) was currently the most common used method to estimate gene expression levels. Subsequently, differential expression analysis between two groups was analyzed using the DESeq2 software (version 1.22.1). The corrected *P* value and $|\log_2 FC|$ were used as the threshold for differentially expressed genes (DEGs). Then, gene ontology (GO), KEGG enrichment analysis and transcription factors (TFs) analysis were performed (Love, Huber, & Anders, 2014; Conesa et al., 2016).

3. Results

3.1. Metabolic profiles

The bulbs of *Lilium Bulbus* collected from the different three planting areas were used for metabolic profiling by the extensively metabolomics method based on UPLC-ESI-MS/MS and databases. Firstly, a database was built using standard products, which contained Q1/Q3/RT information of different substances (Q1: high-resolution mass spectrometry data, Q3: mass spectra fragment information, and RT: retention time). In widely targeted metabolomics method, the Q1/Q3/RT information of different signals detected was compared with the database, combining with secondary mass spectra of the signals to obtain qualitative information of the substances. Finally, a total of 641 metabolites were detected in these three samples, among which 556, 565, and 569 metabolites were detected in the bulbs of LD, LB and LL, respectively. Then, 641 metabolites were divided into 15 classes according to their structure types, as listed in Table 1.

Table 1
Classification of detected metabolites in bulbs of LD, LB and LL.

Type of compounds	Number of compounds
Phenolic acids	122
Lipids	95
Organic acids	73
Amino acids and derivatives	60
Alkaloids	58
Flavonoids	50
Steroids	48
Nucleotides and derivatives	45
Lignans and coumarins	25
Saccharides and alcohols	24
Others	12
Terpenoids	10
Vitamin	10
Quinones	5
Tannins	4

The metabolite ion intensity data of all samples were used to carry out the PCA and HCA. PCA can reveal the overall metabolic differences between different groups and the variability of samples within a group by utilizing several principal components. HCA is based on the similarity of samples, which can reveal the differences between samples as well as the repeatability within sample group. In the Fig. 2A, the PCA result declared an obvious separation from different planting areas, while the duplicate samples were compactly clustered together, which suggested that the experiment was reproducible and reliable. The two principal components PC1 and PC2 were 44.71% and 33.66%, separately, and these two PC cumulative contribution explained 78.37% of the total variability. Additionally, the samples of LD vs LL group and LD vs LB group could be clearly distinguished by PC1 and PC2. The HCA result indicated that metabolites from the same planting area were clustered together, suggesting the reliability of the metabolic profiling data. However, the metabolites in LL and LB contrasted with LD were clearly separated and varied greatly, as shown in Fig. 2B.

3.2. Significantly differential metabolites

To detect significantly differential metabolites (SDMs) between medicinal *Lilium Bulbus* (LB and LL) and edible lily (LD) collected from the different three planting areas, we compared each metabolite ion intensity in LL vs LD group and LB vs LD group, with LD as a control group. In the experiment, the criteria for screening differential metabolites meet the following two aspects, (1) the difference of metabolites between the control group and experimental group with fold change ≥ 2 or fold change ≤ 0.5 ; (2) the metabolites with variable importance in projection ($VIP \geq 1$). According to the above screening criteria, the differences in metabolite accumulated levels among samples can be quickly observed by volcano plots.

The analysis of LB contrasted with LD (Fig. 3A and B) showed 314 SDMs with 190 down-regulating and 124 up-regulating. Among them, phenolic acids, lipids, steroids, organic acids and flavonoids ranked the top five in the numbers of up-regulated and down-regulated metabolites. At the same time, most phenolic acids, lipids, and organic acids were down-regulated, while most steroids and flavonoids were up-regulated. A total of 39 steroids were significantly differential, with 33 being up-regulated and six being down-regulated. There were 27 significantly differential flavonoids, of which 17 were up-regulated. In LL vs LD group, there were 298 SDMs as shown in Fig. 3C and D. The top five SDMs in LL vs LD were phenolic acids, lipids, steroids, alkaloids and flavonoids. Among them, a large number of lipids and alkaloids were down-regulated, while flavonoids and steroids were up-regulated, with 24 out of 29 flavonoids and 24 out of 31 steroids being up-

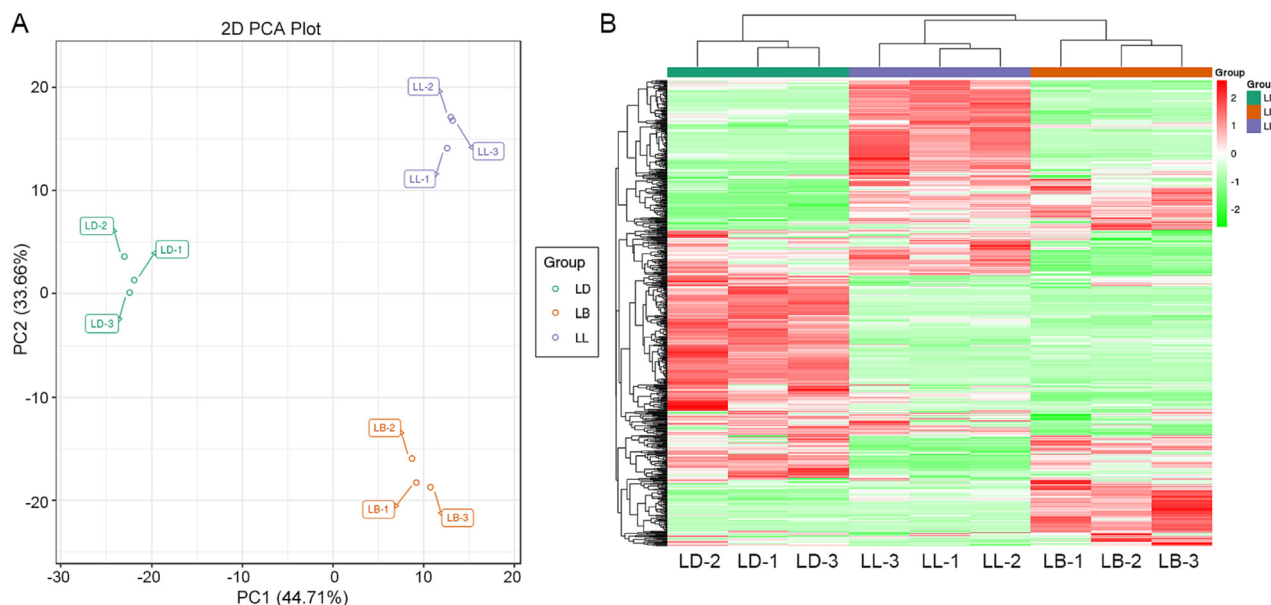


Fig. 2. Principal component analysis (A) and hierarchical clustering heatmap (B) of metabolites from different groups. Red indicates high content and green indicates low content. Data shown are \log_2 FC of metabolite ion intensity.

regulated. The larger the \log_2 FC value is, the greater the difference of this metabolite in different samples is. These significantly differential top 10 up-regulated metabolites in the comparison groups of LB vs LD and LL vs LD were listed as in Table 2 and Fig. 4. The LD vs LB group consisted of four steroidal saponins, five steroid alkaloids, and one sesquiterpenoid saponin, suggesting that the steroids accounted for the largest proportion. The relative contents of these steroids demonstrated extremely variety with FC values from 1.96×10^5 to 5.12×10^6 fold. While three steroidal saponins, one steroid alkaloid, two phenolic acids, two stilbenes, one sesquiterpenoid, and one flavonoid were top 10 up-regulated metabolites in LD vs LL group, with five structure types.

Next, a total of 49 steroidal saponins or steroidal alkaloids detected in LB, LD or LL were analyzed as listed in Table S1 (see in supplementary data). After adjusting the substance identification to level A, the remaining 15 steroidal saponins or steroidal alkaloids did not exist in LD, while they can be detected in LB or LL (Table 3).

3.3. Differentially expressed genes

To explore the molecular basis between medicinal *Lilii Bulbus* and edible lily, we used transcriptomics to identify DEGs in these three groups. More than 12G of raw data were analyzed and filtered in the experiment. At least 80 million clean data was obtained for subsequent analysis by sequencing error rate and GC content distribution check with $Q_{20} \geq 97.38\%$ and $Q_{30} \geq 92.91\%$, indicating that the transcriptome data was highly reliable and could be used for further *de novo* assembly. After assembly, 326 394 unigenes were gained and 95.89% of them distributed between 300 and 2 000 bp lengths. Next, 52 924 DEGs were screened from all samples based on the filter criteria $|\log_2$ FC ≥ 1 and $FDR < 0.05$. Simultaneously, the gene expression level (FPKM) was centralized and standardized to perform Kmeans clustering analysis. The same type of gene exhibited similar variation trend under different experimental treatments. Thus, DEGs were divided into six subclasses based on the gene expression trend, as presented in Fig. 5A. The HCH showed that the genes were clustered together in the same group, while there were obvious differences among these three plants, especially in LB vs LD group

(Fig. 5B). In the comparative experiment, 47 540 DEGs with 23 790 up-regulated genes and 23 750 down-regulated genes in LD vs LB group and 18 958 DEGs with 3 977 up-regulated genes and 14 981 down-regulated genes in LD vs LL group were identified, respectively.

Then, the DEGs were analyzed based on KEGG, NR, Swiss-Prot, KOG/COG, GO, Trembl, and Pfam database to obtain the annotation information. GO analysis of 24 774 DEGs in LD vs LB group and 10 658 DEGs in LD vs LL group were classified in three major GO categories, comprising biological process, cellular component and molecular function (Fig. S2 and S3 in supplementary data). The KOG database analysis suggested that DEGs were grouped into 25 functional categories, of which 1 254 DEGs in LD vs LB group and 607 DEGs in LD vs LL group were assigned to the cluster of secondary metabolites biosynthesis, transport and catabolism (see Fig. S4 in supplementary data). KEGG analysis indicated that 15 262 DEGs in LD vs LB group were mapped onto 142 pathways and 6 192 DEGs in LD vs LL group were mapped onto 138 pathways, which were classified into cellular processes, environmental information processing, genetic information processing, metabolism, and organismal systems (see Fig. S5 in supplementary data). However, 6 716 (44%) DEGs and 3 753 (24.59%) DEGs in LD vs LB group as well as 1 823 (45.59%) DEGs and 1 658 (26.78%) DEGs in LD vs LL group were annotated into metabolic pathway and biosynthesis of secondary metabolites, respectively. Among them, the top 20 pathways enriched by DEGs were shown in Fig. 6, including steroid biosynthesis and biosynthesis of amino acids pathways in LD vs LB group as well as phenylpropanoid biosynthesis, isoflavonoid biosynthesis, and flavonoid biosynthesis pathways in LD vs LL group.

Methyl erythritol phosphate (MEP) and mevalonic acid (MVA) signaling pathways are essential routes involving in the biosynthesis of dimethylallyl diphosphate (DMAPP) and isopentenyl diphosphate (IPP). IPP and DMAPP are important precursors for steroidal saponin or steroidal alkaloids. A total of 269 DEGs in LD vs LB group and 111 DEGs in LD vs LL group maybe involve in the biosynthesis of steroids in KEGG enriched pathways (Fig. 7), including terpenoid backbone biosynthesis (ko00900), steroid biosynthesis (ko00100), sesquiterpenoid and triterpenoid biosynthesis (ko00909), and brassinosteroid biosynthesis (ko00905). Among them, steroid

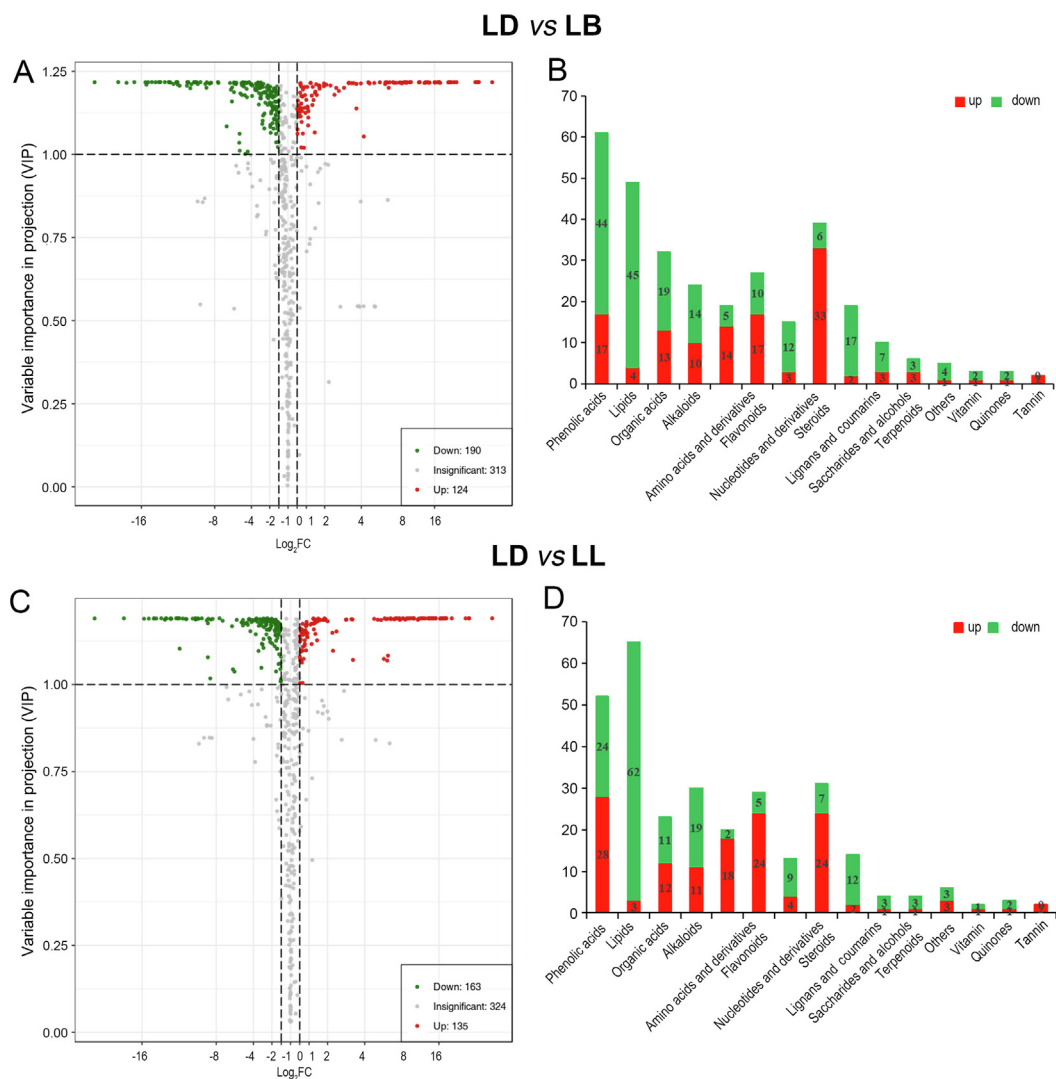


Fig. 3. Analysis of significantly differential metabolites in LB vs LD and LL vs LD, respectively. A, C: volcano plots depicting the up- and down- accumulated metabolites; B, D: numbers of up- and down-accumulated metabolites of different structure types. Metabolites with variable importance in projection (VIP) ≥ 1 and fold change ≥ 2 or fold change ≤ 0.5 were declared significantly.

biosynthesis (ko00100) and brassinosteroid biosynthesis (ko00905) successively contained 80 (0.52%) and 31 (0.2%) DEGs in LD vs LB group, as well as 27 (0.44%) and 17 (0.27%) DEGs in LD vs LL group. The DEGs in the biosynthesis of steroids were more in LD vs LB group than in LD vs LL group. The numbers of some key DEGs detected in biosynthesis of steroids were summarized in Table 4. Among them, the numbers of up- and down-regulated DEGs with clear annotation in LD vs LB group were 62 and 70, respectively. However, there were small amount of DEGs in LD vs LL group, with 17 up-regulated and 38 down-regulated DEGs.

The downstream steps from cholesterol to different steroidal alkaloids and steroidal saponins included hydroxylation, oxidation, transamination, and glycosylation. The screened 43 CYP450 genes from those annotated genes mapping on steroid biosynthesis and brassinosteroid biosynthesis were detected (Table S2 in supplementary data), containing *CYP90B*, *CYP90A1*, *CYP724*, *CYP710A*, and *CYP734A1* (Table 4). In LD vs LB group, the above five CYP450s were all expressed differentially, and the expression levels of *CYP724*, *CYP710A* and *CYP734A1* were higher in LB than LD. In LD vs LL group, *CYP90B*, *CYP90A1* and *CYP734A1* were detected in dif-

ferences, with *CYP90B* being up-regulated. These CYP450s most likely involved in the biosynthesis of steroidal saponins and steroidal alkaloids identified in LB and LL.

3.4. Correlation analysis of transcriptome and metabolome

By comparing the DEGs and SDMs in LL vs LD and LL vs LB groups, great DEGs and SDMs were enriched in the same KEGG pathway, including metabolic pathways, biosynthesis of secondary metabolites, and biosynthesis of amino acids. The correlation analysis of the DEGs and SDMs was carried out in LL vs LD and LL vs LB groups (Fig. 8A and C), which displayed that a total of 116 SDMs were significantly associated with ten thousands of DEGs. Many metabolites were positively or negatively regulated by multiple genes. Furthermore, we analyzed the genes related to top 10 SDMs (Table 2) in LD vs LB and LD vs LL groups, respectively. Pearson correlation coefficient was calculated for metabolome and transcriptome data integration, with correlation filtering threshold of $|cor| > 0.8$ and P value < 0.05 . The relationships between screened genes and the most significant metabolites were visualized by using Cytoscape and the top 10 points with the highest connectivity

Table 2
Top ten up-regulated metabolites of FC values in LB and LL compared with LD.

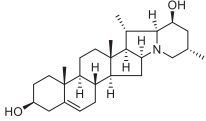
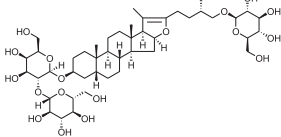
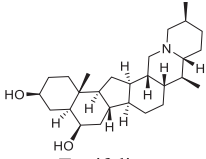
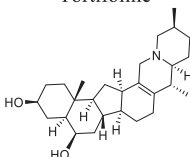
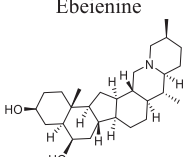
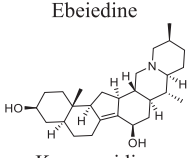
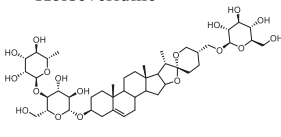
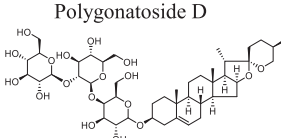
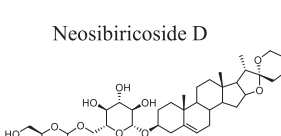
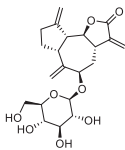
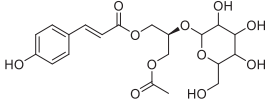
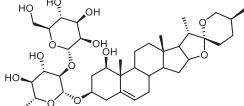
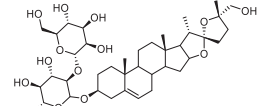
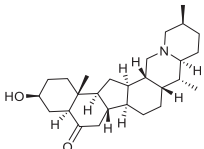
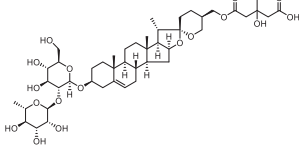
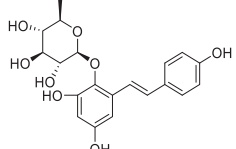
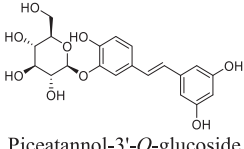
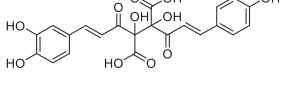
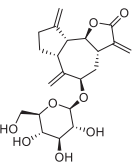
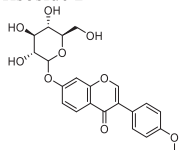
ID	Compounds	Molecular weight	Ionization model	Q1	Q3	Class	log ₂ FC
LB vs LD Lmmp004621	 Leptinidine	413.329	[M + H] ⁺	414.34	414.34	Steroid alkaloid	22.29
pmp001041	 Timosaponin B-III	902.487	[M + H] ⁺	903.49	741.44	Steroidal saponin	20.82
pmp001022	 Tortifoline	415.345	[M + H] ⁺	416.35	416.35	Steroid alkaloid	20.65
pmp001019	 Ebeienine	413.329	[M + H] ⁺	414.34	98.1	Steroid alkaloid	20.45
pmp001021	 Ebeiedine	415.345	[M + H] ⁺	416.35	416.35	Steroid alkaloid	18.39
pmp001020	 Korseveridine	413.329	[M + H] ⁺	414.34	414.34	Steroid alkaloid	18.11
Hmdp003403	 Polygonatoside D	900.472	[M + H] ⁺	901.48	739.43	Steroidal saponin	17.82
Hmdp003423	 Neosibiricoside D	900.472	[M + H] ⁺	901.48	739.43	Steroidal saponin	17.69
Hmdp003401	 Trillin-6'-O-glucoside	738.413	[M + H] ⁺	739.42	577.37	Steroidal saponin	17.58

Table 2 (continued)

ID	Compounds	Molecular weight	Ionization model	Q1	Q3	Class	log ₂ FC
Zmsn001980	 Ixeriside D	408.178	[M + H] ⁻	407.18	203.09	Sesquiterpenoid saponin	17.49
LL vs LD pmn001315	 Regaloside	458.142	[M + H] ⁻	457.14	397.11	Phenolic acid	21.74
pmp000755	 Hydroxyyamogenin-rhamnosyl(1,2)glucoside	738.419	[M + H] ⁺	739.43	595.30	Steroidal saponin	19.26
pmp000093	 Nuatigenin-3-O-[rhamnosyl-(1→2)-glucoside]	738.419	[M + H] ⁺	739.43	595.30	Steroidal saponin	19.23
pmp001018	 Puqiedinone	413.329	[M + H] ⁺	414.34	414.34	Steroid alkaloid	18.88
Hmbp007110	 Brownioside	882.461	[M + H] ⁺	883.47	413.30	Steroidal saponin	17.38
Zmhn101746	 Tetrahydroxy-stilbene-O-glucoside	406.126	[M + H] ⁻	405.12	243.07	Stilbene	16.79
Zmhn001746	 Piceatannol-3'-O-glucoside	406.126	[M + H] ⁻	405.12	243.07	Stilbene	16.75
mad2085	 Caffeoyl- <i>p</i> -coumaroyltartaric acid	458.085	[M + H] ⁻	457.08	295.04	Phenolic acid	16.63

(continued on next page)

Table 2 (continued)

ID	Compounds	Molecular weight	Ionization model	Q1	Q3	Class	log ₂ FC
Zmsn001980		408.178	[M + H] ⁺	407.18	203.09	Sesquiterpenoid	16.46
pme3504	Ixerisoides D  Formononetin-7-O-glycoside	430.126	[M + H] ⁺	431.13	269.08	Flavone	16.46

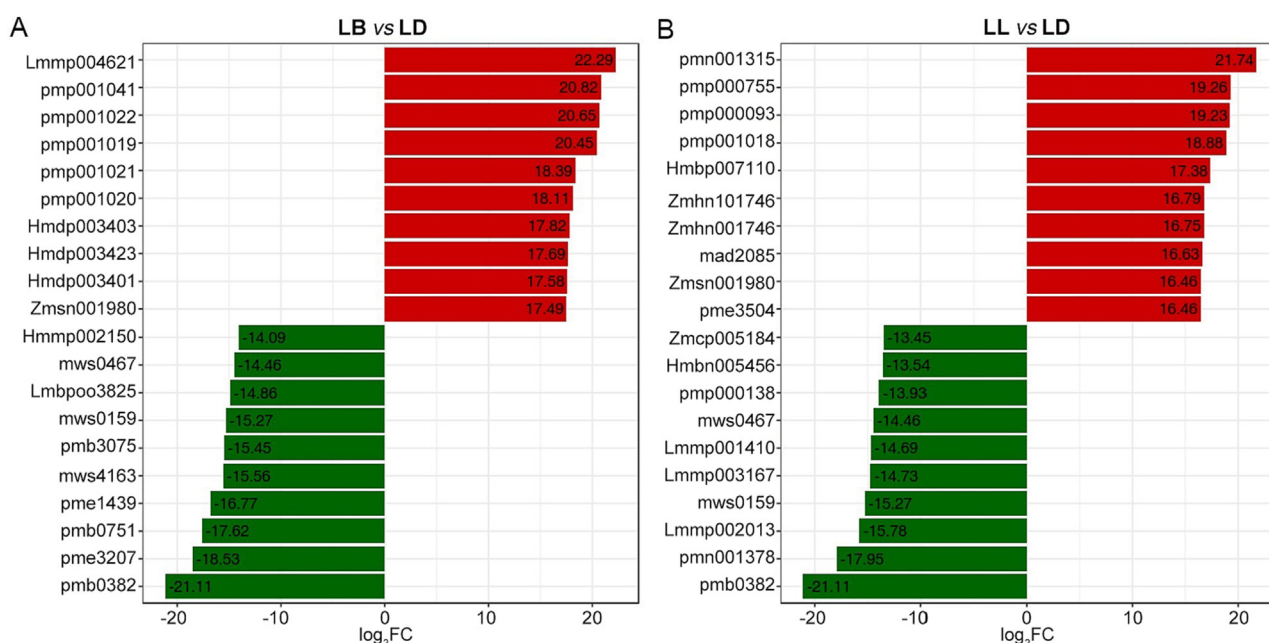


Fig. 4. Top FC change metabolites of up- and down-regulated metabolites in LB vs LD (A) and LL vs LD (B) groups. The x-axis represents value of log₂FC, while y-axis represents serial number of metabolites.

were selected to draw a correlation network diagram, as shown in Fig. 8B and D. While the annotation information of genes was summarized as follows: cluster-10.0: pentatricopeptide repeat-containing protein At1g01970-like isoform X1; cluster-100012.0, cluster-100012.1, and cluster-100012.2: RING-H2 zinc finger protein RHA1; cluster-100020.0: magnesium transporter; cluster-100022.2: beta-1,3-galactosyltransferase; cluster-100027.0: serine/threonine-protein kinase SRPK3; cluster-100028.0: transcription factor TGA; cluster-100032.0: ATP-dependent RNA helicase DDX42; cluster-100004.3: NADPH-ferrihemoprotein reductase; cluster-100.0, cluster-100010.1, cluster-100011.0, cluster-100016.0, and cluster-100037.0: without annotation. Among them, RING-H2 zinc finger proteins play important roles in the regulation of development; magnesium transporters play important roles in coping with magnesium stress, chloroplast development and photosynthesis; beta-1,3-galactosyltransferase is one of the major types of glycosyltransferases; ATP-dependent

RNA helicase DDX42 participates in diverse biological processes involved in RNA metabolism in organisms. However, most of the top 10 genes mentioned above were not mapped on KEGG pathways, and their functions need to be further explored. Among these 20 SDMs as listed in Table 2, there were some studies on the activities of tetrahydroxy-stilbene-O-glucoside (Zmhn101746), such as altering neurogenesis and neuroinflammation, ameliorating cognitive impairments, alleviating ischemic stroke (Gao et al., 2021; Li et al., 2022; Miao et al., 2022; Gao et al., 2023), and so on. However, the investigations of steroidal saponins or steroid alkaloid were relatively few, which needed to further research and explore. Only timosaponin B-III (pmp001041) showed anti-depressive activity (Jiang et al., 2014; Zhang, Wang, Xiong, Huang, & Xue, 2017; Zhong et al., 2019) and puqiedinone (pmp001018) had antimalarial activity (Bora et al., 2023). The anti-depressive activity of timosaponin B-III may be related to the refreshing and calming efficacy of *Lilii Bulbus*.

Table 3
Steroidal saponins and steroid alkaloids present in medicinal *Lilii Bulbus* (LB and LL) but not in edible lily (LD).

Index	Compounds	Class
pmp000092	Nuatigenin-3-O-glucoside	Steroidal saponins
pmp000755	Hydroxy-yamogenin-rhamnosyl(1,2)glucoside	Steroidal saponins
pmp000093	Nuatigenin-3-O-[rhamnosyl-(1 → 2)-glucoside]	Steroidal saponins
Hmbp007110	Brownioside	Steroidal saponins
Hmqn007358	26-O-Glucosylnuatigenin-3-O-rhamnosyl(1 → 4)glucoside	Steroidal saponins
Hmbn006412	26-O-Glu-3β,26-dihydroxy-5-cholesten-16,22-dioxo-3-O-α-rha(1 → 2)-glucoside	Steroidal saponins
Hmbn006860	27-O-[(3S)-3-O-Glu-3-methylglutaroyl]isonarthogenin-3-O-[rha-(1 → 2)]-glucoside	Steroidal saponins
Hmbn006558	27-O-(3-Hydroxy-3-methylglutaroyl)spirost-5-ene-3β,27-diol(isonarthogenin)-3-O-rha-(1 → 2)-O-[glu-(1 → 4)]-glucoside	Steroidal saponins
Hmdp003401	Trillin-6'-O-glucoside	Steroidal saponins
Hmbp003369	Cynatratoside E	Steroidal saponins
Lmmp004621	Leptinidine	Steroid alkaloids
pmp001019	Ebeienine	Steroid alkaloids
pmp001020	Korseveridine	Steroid alkaloids
pmp001030	Yibeinoside A	Steroid alkaloids
pmp001018	Puqiedinone	Steroid alkaloids

4. Discussion

Before the Ming Dynasty, the varieties of medicinal *Lilii Bulbus* were *L. brownii* var. *viridulum* (LB) with white flowers and its varieties. After the Ming Dynasty, *L. lancifolium* (LL), LB and *L. pumilum* DC. (LP) were mixed as sources of *Lilii Bulbus*, but LB is recognized

as a better variety for *Lilii Bulbus* than others and still the mainstream variety. The 1977 edition of the *Chinese Pharmacopoeia* stipulated that the varieties of *Lilii Bulbus* were LL, LB and LP, while LL became the largest source of *Lilii Bulbus*, ranking first (Chinese Pharmacopoeia Commission, 1977; Wang et al., 2018). The change was related to the mature cultivation technology of LL and the

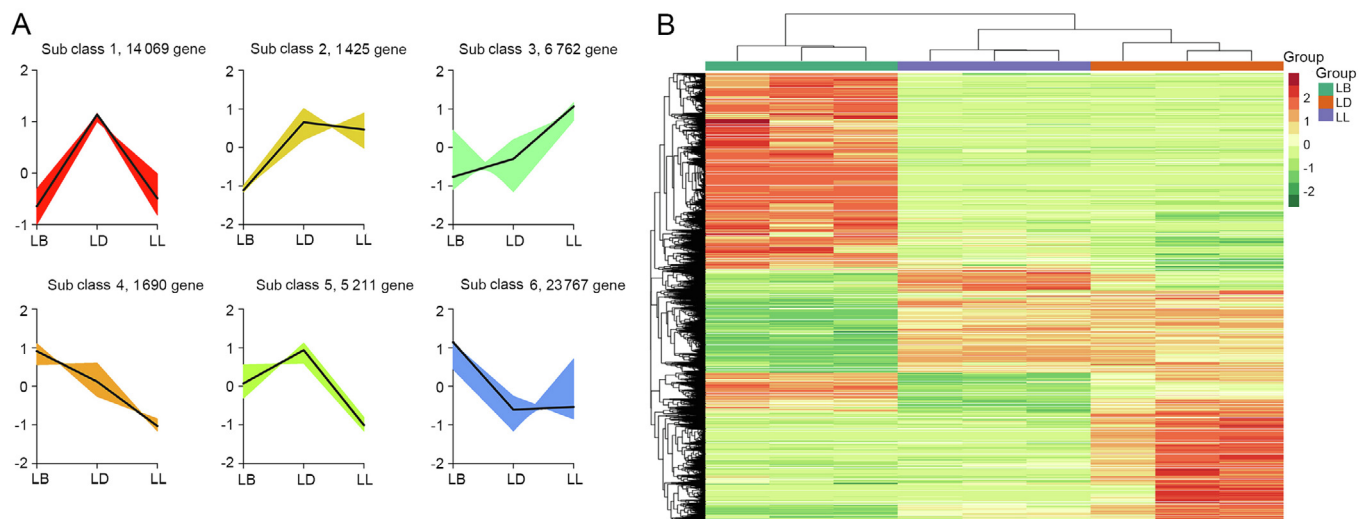


Fig. 5. Differential expression genes cluster analysis in LB, LD and LL. A: Kmeans cluster diagram. The x-axis represents the sample information, while the y-axis represents the expression level of genes (FPKM). B: Hierarchical clustering heatmap. Red indicates high expression and green indicates low expression.

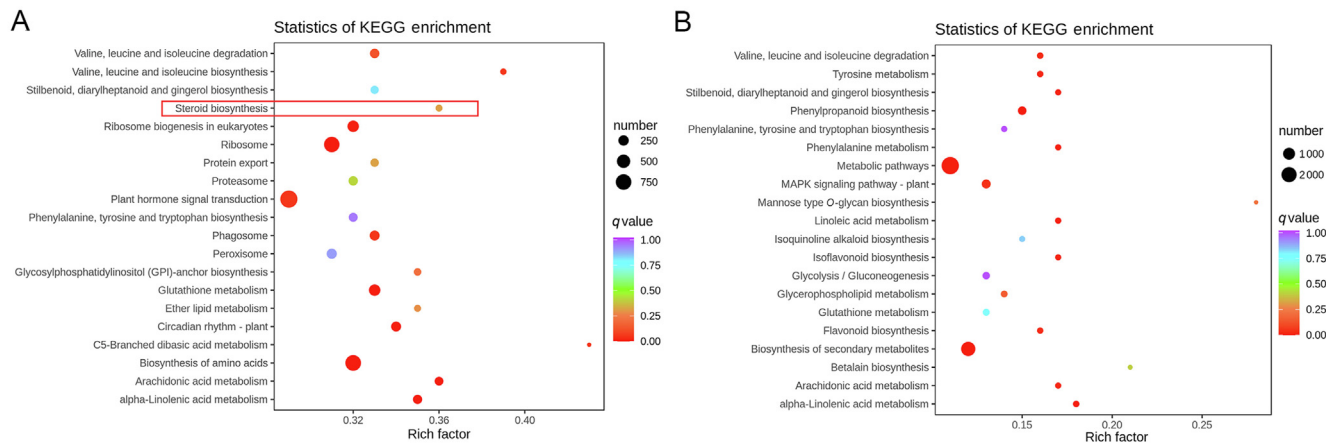


Fig. 6. Top 20 significantly enriched KEGG pathways ($P < 0.05$) of DEGs in LD vs LB (A) and LD vs LL (B). The enriched steroid biosynthesis pathway was labeled by red frame.

rapid growth of production to meet people's drug needs, but that was not consistent with the ancient medicinal situation of *Lilii Bulbus* (Wang et al., 2018; Zhang et al., 2019; Qjin et al., 2022). Until now, the 2020 version of *Chinese Pharmacopoeia* still recorded LL, LB, and LP as the sources of *Lilii Bulbus*, of which LL and LB accounted for 98% in the market as *Lilii Bulbus*. In order to explore the therapeutic material basis of *Lilii Bulbus*, we chose *L. davidii* var. *willmottiae* (LD) used only for food as the control group as well as LL and LB as the experimental groups to clarify the possible functional components of *Lilii Bulbus* by the analysis of metabolome and transcriptome.

In extensively metabolomics experiment, the PCA and HCA results implied that a large number of metabolites were significantly differential between the control group (LD) and the experimental groups (LB and LL) (Fig. 2). Then, the volcano plots analysis

of SDMs indicated that there were more SDMs in LB vs LD group than in LD vs LL group. Among them, most of steroids, flavonoids, and amino acids and derivatives were up-regulated compared with LD, while the amount of flavonoids and steroids was relatively large (Fig. 3). Compared with flavonoids, steroids was a larger proportion of up-regulated metabolites in LD vs LB group, with steroidal saponins and steroidal alkaloids being mainly two kinds of steroidal compounds detected. However, the proportion of up-regulated flavonoids was higher than that of up-regulated steroids in LD vs LL group. The analysis of the top 10 up-regulated SDMs with the highest FC values found that the steroidal saponins and steroidal alkaloids accounted for the largest proportion in LD vs LB group and LD vs LL group. Moreover, the relative contents of these steroidal saponins and steroidal alkaloids demonstrated extremely variety, especially in the LB vs LD group (Fig. 4 and

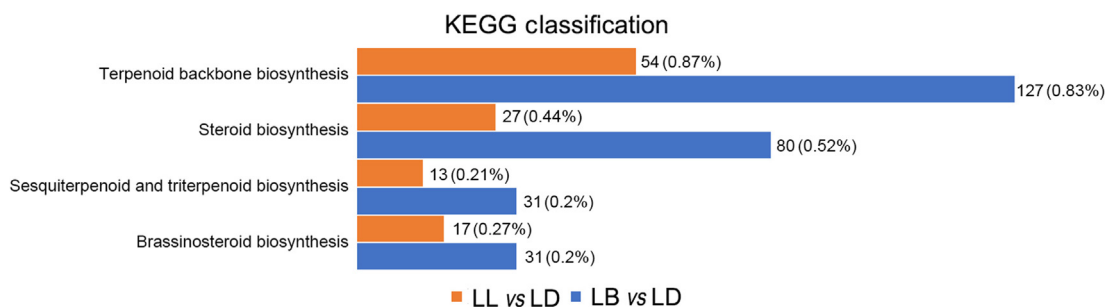


Fig. 7. Numbers of differentially expressed genes involving in biosynthesis of steroids in KEGG classification in comparison group of LB vs LD and LL vs LD, respectively.

Table 4
Numbers of up-regulated and down-regulated DEGs identified in biosynthesis of steroids.

KEGG pathways	Annotation	Enzyme commission number (EC)	LD vs LB		LD vs LL	
			up	down	up	down
Terpenoid backbone biosynthesis	HMGR: hydroxymethylglutaryl-CoA reductase (NADPH)	1.1.1.34	6	8	1	2
	MK: mevalonate kinase	2.7.1.36	1	1	–	–
	PMK: phosphomevalonate kinase	2.7.4.2	1	1	0	1
	MVD: diphosphomevalonate decarboxylase	4.1.1.33	3	3	1	3
	DXR: 1-deoxy-D-xylulose 5-phosphate reductoisomerase	1.1.1.267	0	1	0	1
	CMK: 4-diphosphocytidyl-2-C-methyl-D-erythritol kinase	2.7.1.148	1	2	0	2
	MCS: 2-C-methyl-D-erythritol 2,4-cyclodiphosphate synthase	4.6.1.12	1	5	0	4
	HDR: 4-hydroxy-3-methylbut-2-en-1-yl diphosphate reductase	1.17.7.4	2	4	0	1
	GPPS: geranyl diphosphate synthase	2.5.1.1	1	1	0	1
	SQLE: squalene monooxygenase	1.14.14.17	4	6	0	2
Sesquiterpenoid and triterpenoid biosynthesis	CAS: cycloartenol synthase	5.4.99.8	2	1	–	–
	SMT1: sterol 24-C-methyltransferase	2.1.1.41	5	1	1	0
Steroid biosynthesis and brassinosteroid biosynthesis	CYP51: sterol 14-demethylase	1.14.13.70	2	1	–	–
	FK: Delta14-sterol reductase	1.3.1.70	2	1	2	0
	HDY1: cholesterol Delta-isomerase	5.3.3.5	0	1	0	1
	DWF5: 7-dehydrocholesterol reductase	1.3.1.21	1	1	2	0
	Delta7-sterol 5-desaturase	1.14.19.20	0	1	0	2
	sterol-4alpha-carboxylate 3-dehydrogenase (decarboxylating)	1.1.1.170	6	5	0	3
	steroid 3-oxidase	1.14.-.-	0	1	0	1
	brassinosteroid-6-oxidase 1	1.14.-.-	0	1	0	1
	steroid 5-alpha-reductase	1.3.1.22	2	5	3	2
	Delta24-sterol reductase	1.3.1.72	7	3	2	1
Later stage modifications (CYP450s)	methylsterol monooxygenase 1	–	1	3	0	3
	methylsterol monooxygenase 2	–	2	3	0	3
	CYP90B: steroid 22-alpha-hydroxylase	1.14.14.178	6	6	5	2
	CYP90A1: cytochrome P450 family 90 subfamily A polypeptide 1	1.14.19.79	1	2	0	1
	CYP724: cytochrome P450 family 724 subfamily B polypeptide 1	1.14.13.-	1	0	–	–
	CYP710A: sterol 22-desaturase	1.14.19.41	2	1	–	–
	CYP734A1: PHYB activation tagged suppressor 1	1.14.-.-	2	1	0	1

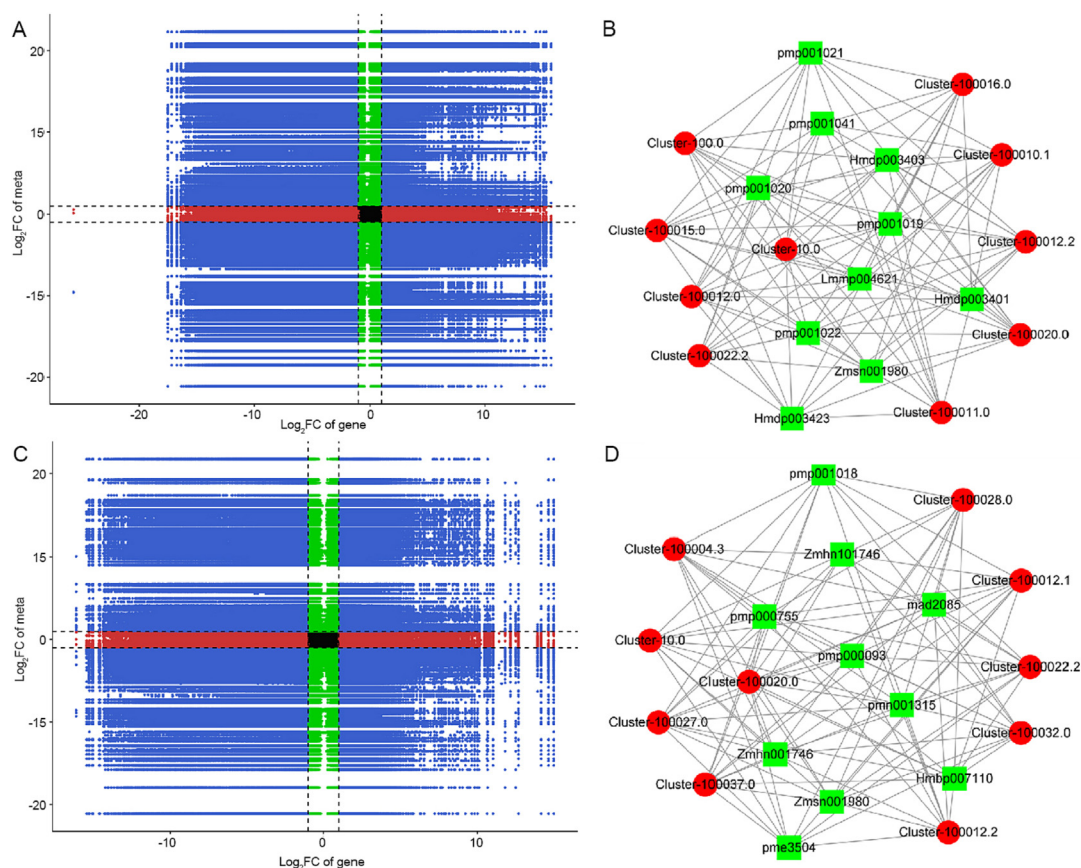


Fig. 8. Nine quadrant diagram showing correlation of differentially expressed genes and differentially accumulated metabolites in LB vs LD (A) and LL vs LD (C) groups. Connection network between differentially expressed genes (red circles) and differentially accumulated metabolites (green square) in LB vs LD (B) and LL vs LD (D) groups.

Table 2). Additionally, 49 steroidal saponins or steroidal alkaloids were detected in all samples. After the substance identification level was adjusted to A level, there were remaining 17 steroidal saponins or steroidal alkaloids. Among them, 15 out of 17 compounds did not exist in LD, while they could be detected in LB or LL (Table 3).

Based on the metabolomics experimental analysis, it is speculated that the up-regulated flavonoids and steroids may be the major functional components of medicinal lilies (LB and LL). However, flavonoids almost existed in all plants, while steroidal saponins and steroidal alkaloids were representative components of *Lilium* plants. Therefore, the steroidal saponins and steroidal alkaloids in medicinal lilies (LB and LL) may play an important role in the drug efficacy contrasted with edible lily (LD). However, there are a few investigations on the biological activities of these steroidal saponins and steroidal alkaloids. For example, puqiedinone (pmp001018) shows antimalarial activity (Bora et al., 2023), and yibeinoside A have both anti red blood cell acetylcholinesterase and anti-plasma butyrylcholinesterase activities (Lin, Ji, Li, Fang, & Jiang, 2006). Thus, steroidal saponins and steroidal alkaloids require further and deeper research to provide a fundamental basis for the interpretation of *Lilii Bulbus* efficacy.

The HCA of transcriptome indicated that there were significant differences in LB vs LD group and LD vs LL group, while the difference between LL and LD varied slightly (Fig. 5). The DEGs in LB vs LD group were greater than LD vs LL group. The enriched top 20 pathways included steroid biosynthesis pathway only in LD vs LB group, without in LD vs LL group (Fig. 6). The biosynthesis pathway of steroids was summarized through the detected related genes, and more DEGs were detected in LD vs LB group, but fewer

in LD vs LL group, as shown in Fig. 7 and Table 4. Most of enzymes involving in the biosynthesis pathway of steroids comprised up-regulated and down-regulated genes.

Phytosterols, also called plant sterols, have been reported over 250 different sterols. The most abundant and representative are sitosterol, stigmasterol and campesterol (precursor of brassinosteroids). While cholesterol level is extremely low in most plant species, but cholesterol is also an important precursor in the biosynthesis of steroids (Yang et al., 2019; Tada, Kojima, Takamura, & Kawashiri, 2022). Brassinosteroids are plant hormones regulating different developmental processes, and they have no other bioactive properties like steroidal saponins or alkaloids. Thus, we focused the downstream steps from cholesterol to differential steroidal glycoalkaloids and steroidal saponins. Previously studies showed that the enzymes involving in the formation of various steroidal saponins and steroidal alkaloids mainly consisted of cytochrome P450 family genes (CYP450s), UDP-glycosyltransferases (UGTs), and Gamma-aminobutyrate aminotransferase (GAME) (Upadhyay, Jeena, Shikha, & Shukla, 2018; Zhao et al., 2018; Yang et al., 2019; Guo et al., 2021; Kumar, Ashrita, Acharya, & Warghat, 2021; Sharma et al., 2021; Lu et al., 2022).

Steroidal saponins and glycoalkaloids are mainly synthesized from cholesterol by oxygenation at the C-16, C-22, and C-26 positions, with cytochrome P450 enzymes playing important roles in catalyzing these transformations. In our study, we screened 43 CYP450 unigenes (see Table S2 in supplementary data) from those annotated genes mapping on steroid biosynthesis and brassinosteroid biosynthesis, which were closely related to CYP90B, CYP90A1, CYP724, CYP710A, and CYP734A1. Among them, CYP90B1

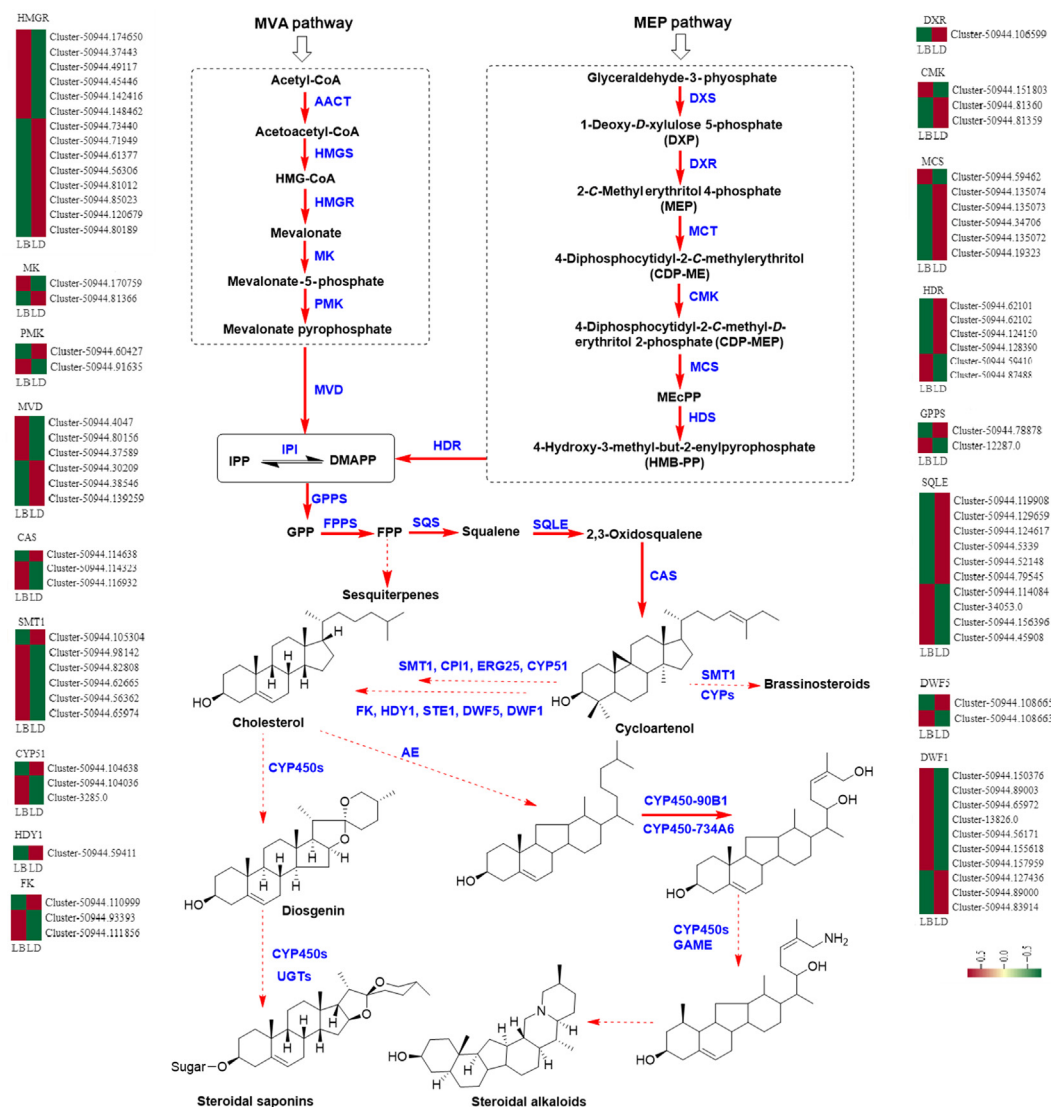


Fig. 9. Putative biosynthesis pathway leading to steroidal saponins and steroidal alkaloids.

and *CYP734A1* are thought to participate in the biosynthesis of steroidal saponins in angiosperms. While the hydroxylation of cholesterol to 22-hydroxycholesterol is possibly catalyzed by *CYP90B1* and the hydroxylation of C-16 and C-26 may be catalyzed by *CYP734A1* (Yang et al., 2019). Additionally, arabidopsis *CYP90B1* catalyses the early C-22 hydroxylation of C₂₇, C₂₈ and C₂₉ sterols (Fujita et al., 2006); while *CYP90B* and *CYP724B* are also steroid C-22 hydroxylase (Ohnishi, Yokota, & Mizutani, 2009). For example, *PpCYP90B27* is demonstrated to catalyze the hydroxylation of cholesterol to produce 22(R)-hydroxycholesterol (Yin, Gao, Zhang, & Gao, 2018). *CYP90B27*, *CYP94N1*, *GABAT1*, and *CYP90G1* catalyze steroid alkaloid biosynthesis in *V. californicum* to form verazine (Augustin et al., 2015); Arabidopsis *CYP710A1* and tomato *CYP710A11* exhibits C-22 desaturase activity with β-sitosterol to produce stigmasterol, and arabidopsis *CYP710A2* is able to produce brassicasterol and stigmasterol from 24-*epi*-campesterol and β-sitosterol, respectively (Morikawa et al., 2006). Therefore, these detected CYP450s (*CYP90B*, *CYP90A1*, *CYP724*, *CYP710A*, and *CYP734A1*) most likely involved in the biosynthesis of steroidal saponins and steroidal alkaloids in LB and LL. In LD vs LB group, the above five CYP450s were all expressed differentially, and the

expression levels of *CYP724*, *CYP710A* and *CYP734A1* were higher in LB than LD. While only *CYP90B*, *CYP90A1* and *CYP734A1* were detected in differences between LD and LL, with *CYP90B* being up-regulated in LL. However, it is unfortunately that UGT and GAME genes were not annotated in the detected genes, possibly due to low content or database not annotated. In reported literature, *DzGT1* is a UDP-rhamnosyltransferase that can catalyze the trillin to form trillin-3'-*O*-glucoside (Li et al., 2021). Finally, the putative biosynthesis pathway leading to steroidal saponins and steroidal alkaloids was presented in Fig. 9. Simultaneously, the relative expression levels of these genes in LD vs LB group also were shown with the form of heat maps.

5. Conclusion

The analysis of metabolome suggested that the steroidal saponins and steroidal alkaloids were significantly up-regulated in LB and LL groups compared with LD group, especially in LB group with the higher content and more numbers. The transcriptome analysis displayed 47 540 DEGs in LD vs. LB group and 18 958 DEGs in LD vs. LL group. There was significant difference in LB vs LD group and LB

vs. LL group, while the difference between LL and LD varied slightly. Additionally, some CYP450 genes likely involving in the biosynthesis of steroidal saponins and steroidal alkaloids were detected. Comparing with LD, *CYP724*, *CYP710A*, *CYP734A1* and *CYP90B* were up-regulated in LB and LL, respectively. Thus, we speculated that steroidal saponins and steroidal alkaloids were likely to be the representative functional components of *Lilii Bulbus* and the above results may be the reason that LB with white flowers is the mainstream variety of *Lilii Bulbus*, which could provide some references for the use of medicinal *Lilii Bulbus* variety. We recommend that *L. brownii* var. *viridulum* should be selected as the mainstream variety of *Lilii Bulbus* used in the research and development of classic famous formula. Additionally, the metabolites with the most significant difference can provide a basis for distinguishing medicinal lily from edible lily, which may be used as a quality marker. It is very important to classify the species of *Lilium* for their clinical usage.

CRedit authorship contribution statement

Wenjun Wei: Conceptualization, Investigation, Formal analysis, Methodology, Data curation, Writing – original draft, Writing – review & editing, Visualization. **Tao Guo:** Supervision, Project administration, Funding acquisition. **Wenguang Fan:** Data curation. **Mengshan Ji:** Methodology, Visualization. **Yu Fu:** Investigation, Data curation. **Conglong Lian:** Data curation. **Suiqing Chen:** Supervision, Data curation. **Wenjing Ma:** Data curation. **Wenfeng Ma:** Data curation. **Shuying Feng:** Supervision, Project administration.

Declaration of Competing Interest

The authors declare that they have no known competing financial interests or personal relationships that could have appeared to influence the work reported in this paper.

Acknowledgments

This research was funded by 2022 Provincial Science and Technology Research and Development Plan United Fund (No. 222301420075), Henan Provincial High-Level Talents International Training Funding Project (No. 2021-72).

Appendix A. Supplementary data

Supplementary data to this article can be found online at <https://doi.org/10.1016/j.chmed.2023.10.004>.

References

- Augustin, M. M., Ruzicka, D. R., Shukla, A. K., Augustin, J. M., Starks, C. M., O'Neil-Johnson, M., McKain, M. R., Evans, B. S., Barrett, M. D., Smithson, A., Wong, G. K., Deyholos, M. K., Edger, P. P., Pires, J. C., Leebens-Mack, J. H., Mann, D. A., & Kutchan, T. M. (2015). Elucidating steroid alkaloid biosynthesis in *Veratrum californicum*: Production of verazine in Sf9 cells. *The Plant Journal*, 82(6), 991–1003.
- Bora, P. S., Agrawal, P., Kaushik, N. K., Puri, S., Sahal, D., & Sharma, U. (2023). Antiplasmodial activity of the bulbs of *Fritillaria cirrhosa* D. Don (Syn: *Fritillaria roylei* Hook.): UPLC-IM-Q-TOF-MS/MS-based biochemometric approach for the identification of marker compounds. *Journal of Ethnopharmacology*, 310, 116389.
- Conesa, A., Madrigal, P., Tarazona, S., Gomez-Cabrero, D., Cervera, A., McPherson, A., Szcześniak, M. W., Gaffney, D. J., Elo, L. L., Zhang, X., & Mortazavi, A. (2016). A survey of best practices for RNA-seq data analysis. *Genome Biology*, 17(1), 13.
- Di, R., Murray, A. F., Xiong, J., Esposito, D., Komarnytsky, S., Gianfagna, T. J., & Munafa, J. P., Jr. (2020). Lily steroidal glycoalkaloid promotes early inflammatory resolution in wounded human fibroblasts. *Journal of Ethnopharmacology*, 258, 112766.
- Esposito, D., Munafa, J. P., Jr., Lucibello, T., Baldeon, M., Komarnytsky, S., & Gianfagna, T. J. (2013). Steroidal glycosides from the bulbs of Easter lily (*Lilium longiflorum*

- Thunb.) promote dermal fibroblast migration *in vitro*. *Journal of Ethnopharmacology*, 148(2), 433–440.
- Fujita, S., Ohnishi, T., Watanabe, B., Yokota, T., Takatsuto, S., Fujioka, S., Yoshida, S., Sakata, K., & Mizutani, M. (2006). Arabidopsis *CYP90B1* catalyses the early C-22 hydroxylation of C27, C28 and C29 sterols. *The Plant Journal*, 45(5), 765–774.
- Gao, D., Chen, C., Huang, R., Yang, C. C., Miao, B. B., Li, L., & Zhang, L. (2021). Tetrahydroxy stilbene glucoside ameliorates cognitive impairments and pathology in APP/PS1 transgenic mice. *Current Medical Science*, 41(2), 279–286.
- Gao, D., Hao, J. P., Li, B. Y., Zheng, C. C., Miao, B. B., Zhang, L., Li, Y. L., Li, L., Li, X. J., & Zhang, L. (2023). Tetrahydroxy stilbene glucoside ameliorates neuroinflammation for Alzheimer's disease via cGAS-STING. *European Journal of Pharmacology*, 953, 175809.
- Guo, S. Y., Yin, Y., Lei, T., Shi, Y. H., Gao, W., Zhang, X. N., & Li, J. (2021). A cycloartenol synthase from the steroidal saponin biosynthesis pathway of *Paris polyphylla*. *Journal of Asian Natural Products Research*, 23(4), 353–362.
- Jiang, W., Guo, J., Xue, R., Zhu, K., Li, Z., Chen, M., & Huang, C. (2014). Anti-depressive activities and biotransformation of timosaponin B-III and its derivatives. *Natural Product Research*, 28(18), 1446–1453.
- Kumar, P., Ashrita Acharya, V., & Warghat, A. R. (2021). Comparative transcriptome analysis infers bulb derived *in vitro* cultures as a promising source for sipeimine biosynthesis in *Fritillaria cirrhosa* D. Don (Liliaceae, syn. *Fritillaria roylei* Hook.)-High value Himalayan medicinal herb. *Phytochemistry*, 183, 112631.
- Li, J., Mosongo, I., Li, H., Wu, Y., Li, C., Yang, S., & Zhang, Y. (2021). Identification and characterization of a trillin rhamnosyltransferase from *Dioscorea zingiberensis*. *Frontiers in Plant Science*, 12, 713036.
- Li, M., Lu, W., Meng, Y., Zhang, W., Wang, F., Sun, L., & Xu, Y. (2022). Tetrahydroxy stilbene glucoside alleviates ischemic stroke by regulating conformation-dependent intracellular distribution of PKM2 for M2 macrophage polarization. *Journal of Agricultural and Food Chemistry*, 70(49), 15449–15463.
- Liang, Z. X., Zhang, J. Z., Xin, C., Li, D., Sun, M. Y., & Shi, L. (2022). Analysis of edible characteristics, antioxidant capacities, and phenolic pigment monomers in *Lilium* bulbs native to China. *Food Research International*, 151, 110854.
- Lin, B. Q., Ji, H., Li, P., Fang, W., & Jiang, Y. (2006). Inhibitors of acetylcholine esterase *in vitro*-screening of steroidal alkaloids from *Fritillaria* species. *Planta Medica*, 72(9), 814–818.
- Love, M. I., Huber, W., & Anders, S. (2014). Moderated estimation of fold change and dispersion for RNA-seq data with DESeq2. *Genome Biology*, 15(12), 550.
- Lu, Q., Li, R., Liao, J., Hu, Y., Gao, Y., Wang, M., Li, J., & Zhao, Q. (2022). Integrative analysis of the steroidal alkaloids distribution and biosynthesis of bulbs *Fritillariae Cirrhosae* through metabolome and transcriptome analyses. *BMC Genomics*, 23(1), 511.
- Matsuo, Y., Takaku, R., & Mimaki, Y. (2015). Novel steroidal glycosides from the bulbs of *Lilium pumilum*. *Molecules*, 20(9), 16255–16265.
- Miao, B. B., Gao, D., Hao, J. P., Li, Y. L., Li, L., Wang, J. B., Xiao, X. H., Yang, C. C., & Zhang, L. (2022). Tetrahydroxy stilbene glucoside alters neurogenesis and neuroinflammation to ameliorate radiation-associated cognitive disability via AMPK/Tet2. *International Immunopharmacology*, 110, 108928.
- Mimaki, Y., & Sashida, Y. (1990). Steroidal saponins and alkaloids from the bulbs *Lilium brownii* var. *colchesteri*. *Chemical and Pharmaceutical Bulletin*, 38(11), 3055–3059.
- Morikawa, T., Mizutani, M., Aoki, N., Watanabe, B., Saga, H., Saito, S., Oikawa, A., Suzuki, H., Sakurai, N., Shibata, D., Wadano, A., Sakata, K., & Ohta, D. (2006). Cytochrome P450 CYP710A encodes the sterol C-22 desaturase in *Arabidopsis* and tomato. *The Plant Cell*, 18(4), 1008–1022.
- Munafa, J. P., Jr., & Gianfagna, T. J. (2015). Chemistry and biological activity of steroidal glycosides from the *Lilium* genus. *Natural Product Reports*, 32(3), 454–477.
- Ohnishi, T., Yokota, T., & Mizutani, M. (2009). Insights into the function and evolution of P450s in plant steroid metabolism. *Phytochemistry*, 70(17–18), 1918–1929.
- Qin, Y., Jin, J., Zhou, R. R., Fang, L. Z., Liu, H., Zhong, C., Xie, Y., Liu, P. A., Qin, Y. H., & Zhang, S. H. (2022). Integrative analysis of metabolome and transcriptome provide new insights into the bitter components of *Lilium lancifolium* and *Lilium brownii*. *Journal of Pharmaceutical and Biomedical Analysis*, 215, 114778.
- Sharma, B., Seth, R., Thakur, S., Parmar, R., Masand, M., Devi, A., Singh, G., Dhyani, P., Choudhary, S., & Sharma, R. K. (2021). Genome-wide transcriptional analysis unveils the molecular basis of organ-specific expression of isosteroidal alkaloids biosynthesis in critically endangered *Fritillaria roylei* Hook. *Phytochemistry*, 187, 112772.
- Si, Y., Chen, X., Guo, T., Wei, W., Wang, L., Zhang, F., Sun, X., & Liu, M. (2022a). Comprehensive 16S rDNA sequencing and LC-MS/MS-based metabolomics to investigate intestinal flora and metabolic profiles of the serum, hypothalamus and hippocampus in p-chlorophenylalanine-induced insomnia rats treated with *Lilium brownie*. *Neurochemical Research*, 47(3), 574–589.
- Si, Y., Wei, W., Chen, X., Xie, X., Guo, T., Sasaki, Y., Zhang, Y., Wang, L., Zhang, F., & Feng, S. (2022b). A comprehensive study on the relieving effect of *Lilium brownii* on the intestinal flora and metabolic disorder in p-chlorophenylalanine induced insomnia rats. *Pharmaceutical Biology*, 60(1), 131–143.
- Sim, W. S., Choi, S. I., Jung, T. D., Cho, B. Y., Choi, S. H., Park, S. M., & Lee, O. H. (2020). Antioxidant and anti-inflammatory effects of *Lilium lancifolium* bulbs extract. *Journal of Food Biochemistry*, 44(5), 13176.
- Tada, H., Kojima, N., Takamura, M., & Kawashiri, M. (2022). Sitosterolemia. *Advances in Clinical Chemistry*, 110, 145–169.
- Tang, Y. C., Liu, Y. J., He, G. R., Cao, Y. W., Bi, M. M., Song, M., Yang, P. P., Xu, L. F., & Ming, J. (2021). Comprehensive analysis of secondary metabolites in the

- extracts from different lily bulbs and their antioxidant ability. *Antioxidants*, 10 (10), 1634.
- Thévenot, E. A., Roux, A., Xu, Y., Ezan, E., & Junot, C. (2015). Analysis of the human adult urinary metabolome variations with age, body mass index, and gender by implementing a comprehensive workflow for univariate and OPLS statistical analyses. *Journal of Proteome Research*, 14(8), 3322–3335.
- Upadhyay, S., Jeena, G. S., Shikha & Shukla, R. K. (2018). Recent advances in steroidal saponins biosynthesis and *in vitro* production. *Planta*, 248(3), 519–544.
- Wang, C. H., Shu, S., Yin, F. J., Zhao, J. F., Zhang, Z. W., Liu, X., & Zhan, Z. L. (2018). Textual research on origin and genuine of *Lilii Bulbus*. *China Journal of Chinese Materia Medica*, 43(8), 1732–1736.
- Wang, F., Wang, W., Niu, X., Huang, Y., & Zhang, J. (2018). Isolation and structural characterization of a second polysaccharide from bulbs of lanzhou lily. *Applied Biochemistry and Biotechnology*, 186(3), 535–546.
- Wei, C., Liang, G., Guo, Z., Wang, W., Zhang, H., Liu, X., Yu, S., Xiong, L., & Lou, J. (2013). A novel integrated method for large-scale detection, identification, and quantification of widely targeted metabolites: Application in the study of rice metabolomics. *Molecular Plant*, 6(6), 1769–1780.
- Wu, X., Hou, J., Zhang, Z., Zhang, Z., Chen, L., Ni, H., Qian, Y., Wu, W., Long, H., Zhang, L., Li, F., Lei, M., Huang, Y., Guo, D., & Wu, W. (2022). In-depth exploration and comparison of chemical constituents from two *Lilium* species through offline two-dimensional liquid chromatography combined with multimode acquisition of high-resolution mass spectrometry. *Journal of Chromatography A*, 1670, 462980.
- Yang, L. P., Guo, X. D., Ji, J., Hu, H. F., Xi, S. Y., Huang, Y. F., Ma, X. H., & Jin, L. (2023). Research progress on mechanism of *Lilii Bulbus* color change and control. *Chinese Traditional and Herbal Drugs*, 54(6), 1978–1985.
- Yang, Z., Yang, L., Liu, C., Qin, X., Liu, H., Chen, J., & Ji, Y. (2019). Transcriptome analyses of *Paris polyphylla* var. *chinensis*, *Ypsilandra thibetica*, and *Polygonatum kingianum* characterize their steroidal saponin biosynthesis pathway. *Fitoterapia*, 135, 52–63.
- Yin, Y., Gao, L., Zhang, X., & Gao, W. (2018). A cytochrome P450 monooxygenase responsible for the C-22 hydroxylation step in the *Paris polyphylla* steroidal saponin biosynthesis pathway. *Phytochemistry*, 156, 116–123.
- Zhang, W., Wang, J. L., Zhang, Z. J., Peng, H. S., Zhang, Z. L., & Yang, H. J. (2019). Herbal textual research on traditional Chinese medicine “Baihe” (*Lilii Bulbus*). *China Journal of Chinese Materia Medica*, 44(22), 5007–5011.
- Zhang, X. L., Wang, L., Xiong, L., Huang, F. H., & Xue, H. (2017). Timosaponin B-III exhibits antidepressive activity in a mouse model of postpartum depression by the regulation of inflammatory cytokines, BDNF signaling and synaptic plasticity. *Experimental and Therapeutic Medicine*, 14(4), 3856–3861.
- Zhao, Q., Li, R., Zhang, Y., Huang, K., Wang, W., & Li, J. (2018). Transcriptome analysis reveals *in vitro*-cultured regeneration bulbs as a promising source for targeted *Fritillaria cirrhosa* steroidal alkaloid biosynthesis. *3 Biotech*, 8(4), 191.
- Zhong, M., Tian, X., Chen, S., Chen, M., Guo, Z., Zhang, M., Zheng, G., Li, Z., Shi, Z., Wang, G., Gao, H., Liu, F., & Huang, C. (2019). Identifying the active components of Baihe-Zhimu decoction that ameliorate depressive disease by an effective integrated strategy: A systemic pharmacokinetics study combined with classical depression model tests. *Chinese Medicine*, 14, 37.
- Zhou, J., An, R., & Huang, X. (2021). Genus *Lilium*: A review on traditional uses, phytochemistry and pharmacology. *Journal of Ethnopharmacology*, 270(6), 113852.
- Zhou, Z. L., Feng, Z. C., Fu, C. Y., Zhang, H. L., & Xia, J. M. (2012). Steroidal and phenolic glycosides from the bulbs of *Lilium pumilum* DC and their potential Na⁺-K⁺ ATPase inhibitory activity. *Molecules*, 17(9), 10494–10502.